

RSC Advances



This is an *Accepted Manuscript*, which has been through the Royal Society of Chemistry peer review process and has been accepted for publication.

Accepted Manuscripts are published online shortly after acceptance, before technical editing, formatting and proof reading. Using this free service, authors can make their results available to the community, in citable form, before we publish the edited article. This *Accepted Manuscript* will be replaced by the edited, formatted and paginated article as soon as this is available.

You can find more information about *Accepted Manuscripts* in the [Information for Authors](#).

Please note that technical editing may introduce minor changes to the text and/or graphics, which may alter content. The journal's standard [Terms & Conditions](#) and the [Ethical guidelines](#) still apply. In no event shall the Royal Society of Chemistry be held responsible for any errors or omissions in this *Accepted Manuscript* or any consequences arising from the use of any information it contains.

A colorimetric Boolean INHIBIT logic gate for the determination of sulfide based on citrate-capped gold nanoparticles

Hao-Hua Deng,^{a,b} Gang-Wei Wu,^{a,c} Xiao-Qing Lin,^{a,b} Xiong-Wei Xu,^d Ai-Lin Liu,^{a,b} Xing-Hua Xia,^e and Wei Chen^{a,b*}

^a Department of Pharmaceutical Analysis, Fujian Medical University, Fuzhou 350004, China

^b Nano Medical Technology Research Institute, Fujian Medical University, Fuzhou 350004, China

^c Department of Pharmacy, Fujian Provincial Hospital, Fuzhou 350001, China

^d Department of Pharmacy, First Affiliated Hospital, Fujian Medical University, Fuzhou 350005, China

^e State Key Laboratory of Analytical Chemistry for Life Science, School of Chemistry and Chemical Engineering, Nanjing University, Nanjing 210093, China.

* Corresponding author. Tel./fax: +86 591 22862016.

E-mail address: chenandhu@163.com (W. Chen).

Hao-Hua Deng and Gang-Wei Wu contributed equally to this work.

1 **Abstract**

2 Herein, we designed a noncommutative logic gate (INHIBIT gate) by utilizing
3 citrate-capped AuNPs as a signal transducer and S^{2-} and TU as mechanical activators
4 and devised a colorimetric sensor for inexpensive, label-free, rapid, sensitive and
5 selective determination of S^{2-} . Under the optimum conditions, 4 μM S^{2-} could induce a
6 significant color change which can be directly recognized by naked eyes. The
7 calibration curve for the absorbance ratios of A_{680}/A_{520} against S^{2-} concentration was
8 linear in the range from 2 to 9 μM and the RSD was 1.3% for the determination of 4
9 μM S^{2-} (n=6). Moreover, this logic gate was successfully applied for sensing S^{2-} in
10 various practical samples, implying its wide applications in food, environment, and
11 biological system.

12

13 **Introduction**

14 Inorganic anions are ubiquitous in biological systems and play vital roles in
15 industrial, medical, and environmental processes. The design of sensitive and
16 selective probes has long been a focus of research as it can provide on-site, real-time
17 detection and quantification of beneficial and toxic anions. Sulfide (S^{2-}) is an
18 inorganic anion widely present in both natural and waste waters, and it is very
19 detrimental to environment attributed to the releasing of hydrogen sulfide (H_2S),
20 which is a toxic gas with a characteristic malodor of rotten eggs. However, H_2S is of
21 high medical concern recently since it has been demonstrated to be an endogenously
22 produced gaseous signaling molecule other than nitric oxide and carbon monoxide.
23 H_2S can interact directly with downstream protein targets through post-translational
24 cysteine sulfhydration as well as via binding to heme iron centers.^{1,2} Furthermore,
25 researches have indicated that the H_2S level is altered in some diseases, such as
26 Alzheimer's disease and Down's syndrome.^{3,4} Although several strategies have been
27 documented for determining sulfide in the literature,⁵⁻¹⁴ the design of new sensors for
28 sulfide in food chemistry, ecosystem, and biological system is still appealing.

29 In recent years, molecular Boolean logic gates have been extensively studied.
30 Application of logic gates in sensing or biosensing simplify the results of

31 measurement, leaving the determination of analytes in samples either “have” or
32 “none”, or the diagnosis of disease either “yes” or “no”. In this field, colorimetric
33 logic gates based on the high absorption extinction coefficients and strongly
34 distance-dependent optical properties of gold nanoparticles (AuNPs) have become
35 more and more attractive for point-of-use application due to their sensitivity,
36 rapidness, low-cost and especially ease of readout with naked eye. Up to now, various
37 AuNPs-based colorimetric logic gates, such as AND, OR, NOR, and INHIBIT, have
38 been established on the platform of DNAzyme,^{15, 16} aptamer,¹⁷⁻²⁰ and target-ligand
39 coordination.²¹⁻²³ The inputs of most logic gates reported previously have been
40 (bio)molecules and metal ions. However, small anions implemented as input in the
41 design of AuNPs-based colorimetric logic gates are exceedingly scarce.²⁴ Herein, we
42 developed a Boolean logic gate based on citrate-capped AuNPs with S²⁻ and thiourea
43 (TU) as inputs, and devised a colorimetric sensor for the logic sensing of S²⁻ in real
44 samples.

45

46 **Experimental**

47 **Chemical and apparatus**

48 Sodium sulfide (Na₂S·9H₂O), ethylenediaminetetraacetate (EDTA) and chloroauric
49 acid (HAuCl₄·4H₂O) were brought from Aladdin Reagent Company (Shanghai,
50 China). Thiourea (TU) and trisodium citrate were purchased from Sinopharm
51 Chemical Reagent Co. Ltd (Shanghai, China). Other reagents and chemicals were at
52 least analytical reagent grade. Double distilled water was used throughout
53 experiments.

54 The UV-visible spectra of citrate-capped AuNPs were recorded by a Shimadzu
55 UV-2450 spectrophotometer (Shimadzu, Japan).

56 **Synthesis of the AuNPs**

57 All glassware used in the following procedures was cleaned in a bath of freshly
58 prepared solution of HNO₃-HCl (1:3, V/V), rinsed thoroughly in water and dried in air
59 prior to use. AuNPs colloids with an average diameter of 13 nm were prepared
60 according to previously published protocols.²⁵ Briefly, 1 mL of 1% HAuCl₄ solution

61 was dissolved in 100 mL of water and boiled. 3 mL of 1% trisodium citrate solution
62 was quickly added to the refluxed HAuCl_4 solution, resulting in a color change from
63 pale yellow to deep red, indicating the formation of gold nanoparticles. After a
64 continuous reflux for an additional 15 min, the solution was slowly cooled down to
65 room temperature. The wine-red solution of AuNPs was stored at 4 °C in refrigerator.
66 The particle concentration of AuNPs (ca. 3.1 nM) was determined according to Beer's
67 law using an extinction coefficient of ca. $2.7 \times 10^8 \text{ M}^{-1} \text{ cm}^{-1}$ at 520 nm for 13 nm
68 AuNPs.²⁶

69 **Sample pretreatment**

70 For real samples analysis, various real samples including river water, mineral water,
71 tap water, human urine, monosodium glutamate, sugar, and white wine, were tested.
72 River water was collected from the Minjiang River, Fujian Province, China. Tap
73 water was collected from our laboratory. Human urine was collected from a healthy
74 man. Mineral water, monosodium glutamate, sugar, and white wine were collected
75 from the local supermarket. Sample pretreatment process was as follows. For river
76 water, mineral water, and tap water, the collected sample (10 mL) was filtered through
77 a 0.22 μm membrane at first, and then 0.1 mM EDTA was added to the filtrate.
78 Finally, the solution was adjusted to pH 9.0 with 2 M NaOH. For human urine and
79 white wine, the collected sample (10 mL) was directly adjusted to pH 9.0 with 2 M
80 NaOH. For monosodium glutamate and sugar, 0.1 g sample was dissolved in 10 mL
81 water and then the solution was adjusted to pH 9.0 with 2 M NaOH.

82 **Logic test for S^{2-}**

83 Sample solutions with and without standard addition are referred to Spiked and
84 Unspiked, respectively. For Spiked samples, known amounts of S^{2-} were added into
85 samples. The samples were determined according to the following steps. 0.2 mL of
86 the sample solution containing 5 μM TU was mixed with 0.2 mL AuNPs solution.
87 The solution was incubated in a 30 °C water bath for 3 min. The output signals were
88 monitored by naked eyes or UV-visible spectrophotometer.

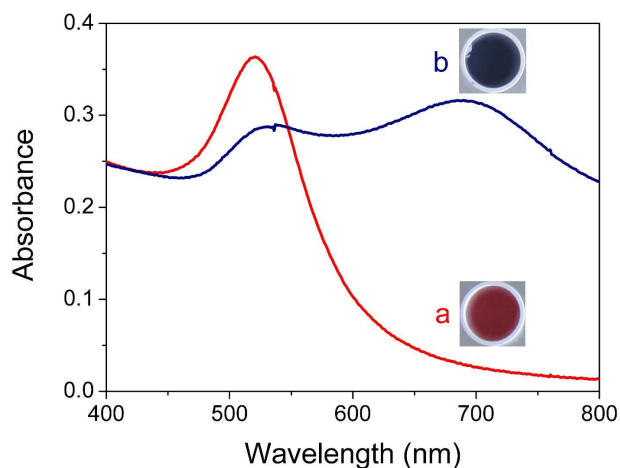
89

90 **Results and discussion**

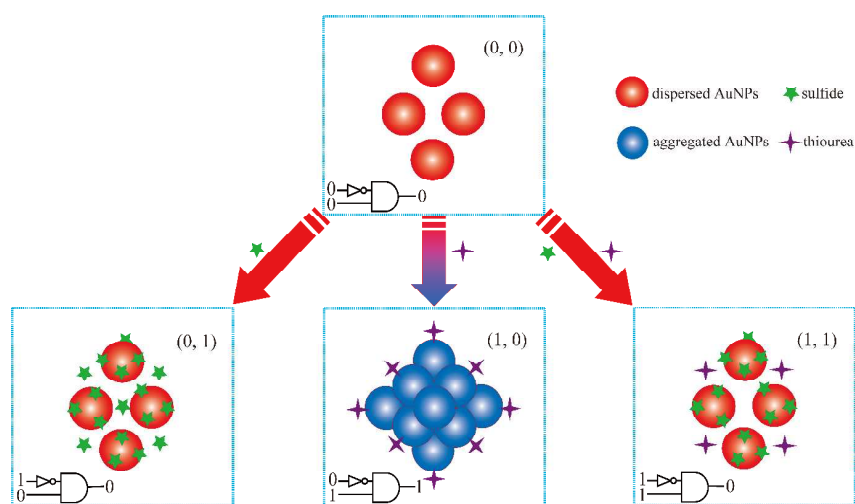
91 **Construction of INHIBIT logic gate**

92 The as-prepared AuNPs showed a distinctive wine-red color with the absorption
93 peak at 520 nm. These AuNPs were relatively stable owing to the electrostatic
94 repulsion invoked by citrate ligands adsorbed on the particles surface. With the
95 addition of TU, the AuNPs rapidly aggregated, along with the consequent shift of the
96 absorption peak to longer wavelength, i.e., 680 nm and a gradual color change from
97 wine-red to blue (Fig. 1). Containing sulfur atom, TU molecule can adsorb on the
98 surface of AuNPs through Au-S bond and replace the original negative citrate ligand.
99 With a pK_a of 2.0, TU remains in the neutral form from pH=2 to pH=10.²⁷ Therefore,
100 the adsorption of TU on the surface of AuNPs results in significantly reduced overall
101 surface charges and increased van der Waals attractive force among nanoparticles,
102 promoting the aggregation of AuNPs. In our experiment, it was found that urea, which
103 is structurally similar to TU, could not induce the aggregation of AuNPs, revealing
104 that S atom rather than amino groups of TU plays a key role in the interaction
105 between TU and AuNPs. Interestingly, the introduction of S^{2-} could prevent the
106 aggregation of AuNPs induced by TU. It is due to the competitive combination of S^{2-} ,
107 which also has high affinity to AuNPs, with TU. Consequently, we expected this
108 phenomenon to act as a INHIBIT logic gate,²⁸ the true output of which is generated
109 when only one input is present without the other input. This logic gate is unique in
110 that it demonstrates noncommutative behavior, i.e. one input has the power to disable
111 the whole system, thus being different from the previous commutative OR, AND, and
112 XOR gates.²⁹ For proof-of-concept, we established a logic gate upon the addition of
113 S^{2-} and TU as the two inputs, and color change of AuNPs as outputs. For input, we
114 defined the presence of S^{2-} or TU as “1”, and the absence as “0”. For output, the
115 well-dispersed red AuNPs solution is defined as “0” and the blue solution with AuNPs
116 aggregates as “1”. Scheme 1 illustrates the working principle of the colorimetric logic
117 gate. With no input or with S^{2-} input alone, citrate-capped AuNPs well dispersed with
118 an output of “0”. With TU input alone, citrate-capped AuNPs aggregated and color of
119 the solution changed from wine-red to blue, giving an output signal of “1”. When the
120 system was subjected to the two inputs together, the introduction of S^{2-} prevented the

121 aggregation of AuNPs induced by TU, and the color output signal was “0”. Therefore,
 122 only the addition of TU would generate a positive output signal “1”, which is in
 123 accord with the proper execution of the INHIBIT logic gate.
 124



125
 126 **Fig. 1** The absorption spectra of (a) citrate-capped AuNPs+9 μM S^{2-} +5 μM TU and (b)
 127 citrate-capped AuNPs+5 μM TU. Inset: the corresponding photographs. Conditions:
 128 pH: 9, and incubation time: 3 min.
 129

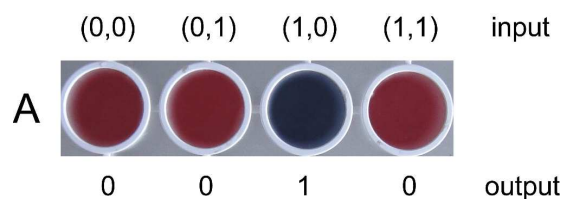


130
 131 **Scheme 1** Schematic illustration of the AuNPs based colorimetric logic gate.
 132

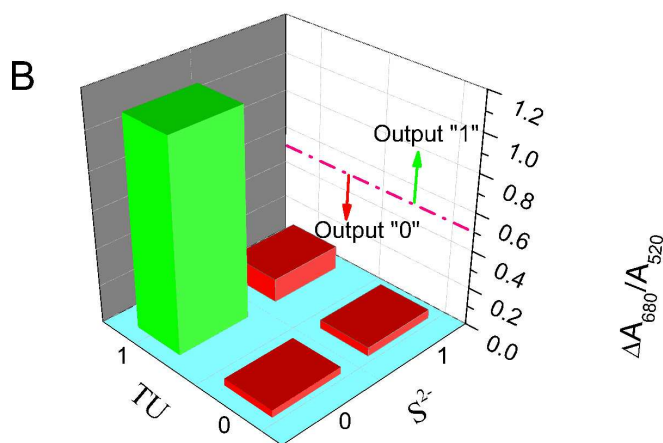
133 Fig. 2A shows the color response of the INHIBIT logic system upon treatment with
 134 S^{2-} and TU inputs. In the presence of TU input (1, 0), the color of the solution turned

135 to blue; while in the absence of both inputs (0, 0), in the presence of S^{2-} input (0, 1), or
 136 both the two inputs (1, 1), the color of the solution remained red. The values of
 137 absorption ratio (A_{680}/A_{520}) toward different inputs were further calculated, with the
 138 output ratio below and above the threshold value of 0.5 defined as "0" and "1",
 139 respectively. It can be seen that only the presence of TU input obtained an output 1,
 140 while the other cases obtained output 0 (Fig. 2B). A truth table is given in Fig. 2C.

141



142



143

Inputs		Outputs	
TU ($5 \mu\text{M}$)	S^{2-} ($9 \mu\text{M}$)	Color of AuNPs	A_{680}/A_{520}
0	0	0 (red)	0 (low)
0	1	0 (red)	0 (low)
1	0	1 (blue)	1 (high)
1	1	0 (red)	0 (low)

144

C

145 **Fig. 2** Operation of the INHIBIT logic. (A) Visual color outputs. (B) Bar-chart
 146 presentation of the absorbance outputs. (C) Truth table corresponding to the INHIBIT

147 logic gate. Conditions: pH: 9, and incubation time: 3 min.

148

149 **TU-AuNPs system for logic sensing of S²⁻**

150 As described above, the logic behavior of the proposed system is INHIBIT, the true
151 output of which is generated when only one input is present without the other input,
152 wherein the red-to-blue color change happens when TU is the only input. According
153 to the experimental results, the introduction of S²⁻ could prevent the aggregation of
154 AuNPs induced by TU, suggesting that TU-AuNPs systems might be a good probe for
155 S²⁻ detection. Next, the TU-AuNPs system for logic sensing of S²⁻ was carefully
156 studied.

157 **Optimization of assay conditions**

158 Media pH influences the stability of citrate-capped AuNPs due to the
159 protonation/deprotonation of the ligand. Since TU is a weak base with a pK_a of 2.0
160 and sulfide exists in three species (H₂S, HS⁻, and S²⁻) in solutions defined by its pK_a,
161 media pH also affects the form of TU and sulfide in aqueous solution. So media pH
162 plays an important role in the interaction among AuNPs, TU and sulfide. We
163 investigated the effect of pH in the range from 5 to 10 and the results are show in Fig.
164 S1. The absorbance of the solution at 680 and 520 nm corresponded to the quantities
165 of aggregated and dispersive AuNPs, respectively. Thus, the molar ratio of aggregated
166 AuNPs to dispersive ones can be expressed by the ratio of the absorbance at 680 nm
167 to that at 520 nm (A_{680}/A_{520}). With the addition of TU that remains in neutral form
168 under the experimental conditions, AuNPs aggregated due to the replacement of the
169 surface bounded negative citrate ligands by neutral TU. This particle aggregation was,
170 however, suppressed by S²⁻, which also has high affinity to AuNPs. It can be seen that
171 the highest increment of the absorbance ratio ($\Delta A_{680}/A_{520}$) was obtained at pH 9. This
172 phenomenon can be explained by the fact that more charged, less protonated species
173 (i.e. HS⁻, S²⁻) formed at higher pH status, which compete with neutral TU molecule
174 for combination with AuNPs resulting in the well-dispersed AuNPs. Hence, all
175 subsequent experiments were carried out with a media pH of 9.

176 Since TU was used as the aggregation promoter of AuNPs, its concentration

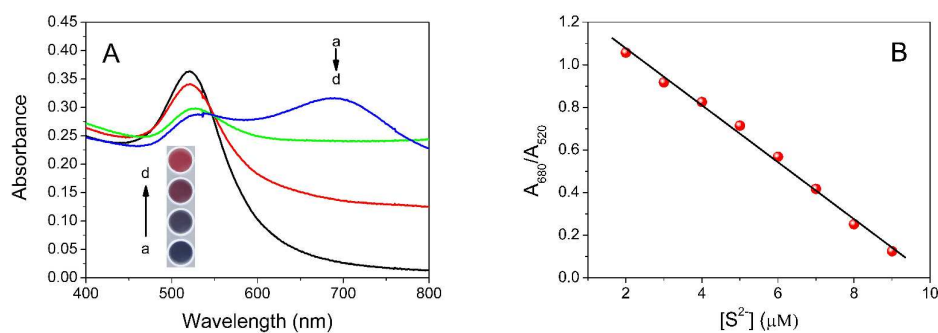
177 directly had an influence on the response of S^{2-} ($\Delta A_{680}/A_{520}$ value). When the
178 concentration of TU was too low, it can not lead to complete aggregation of AuNPs.
179 On the contrary, when the concentration of TU was too high, the sensitivity for S^{2-}
180 determination decreased. The effect of the concentration of TU from 0 to 7 μM was
181 tested. The results showed that the maximum $\Delta A_{680}/A_{520}$ value was readily observed
182 when the concentration of TU was 5 μM (Fig. S2). To obtain high sensitivity, the
183 concentration of TU was selected as 5 μM in the subsequent tests.

184 The kinetics of S^{2-} preventing aggregation of AuNPs induced by TU was
185 investigated. It can be seen from Fig. S3 that the absorbance ratio (A_{680}/A_{520}) first
186 leaped with an increase of the incubation time (0-3 min) and then varied slightly.
187 Hence, all subsequent experiments were carried out with an incubation time of 3 min.

188 **Sensitivity**

189 Under the optimum conditions mentioned above, we evaluated the sensitivity of
190 this new sensor towards S^{2-} . Upon addition of increasing concentrations of S^{2-} , the
191 anti-aggregation ability of S^{2-} for citrate-capped AuNPs became increasingly powerful,
192 along with the absorption peak at 680 nm increased while that at 520 nm decreased
193 (Fig. 3A) and a gradual color change from blue to wine-red (Fig. 3A, inset). It should
194 be noted that 4 μM S^{2-} would induce a distinct color change, which indicated that this
195 low concentration of S^{2-} could be detected by naked eyes. The absorbance ratio
196 (A_{680}/A_{520}) gradually decreased with the addition of increasing concentrations of S^{2-}
197 (Fig. 3B). The calibration curve for the absorbance ratio against S^{2-} concentration was
198 linear in the range from 2 to 9 μM (Fig. 3B, inset) and fit the linear equation
199 $A_{680}/A_{520} = -0.1336C (\mu\text{M}) + 1.3446$ ($r=0.997$). The relative standard deviation was
200 1.3% for the determination of 4 μM S^{2-} ($n=6$).

201



202

203 **Fig. 3** (A) The absorption spectra of sensing systems in absence and presence of
204 different amounts of S^{2-} . The concentrations of S^{2-} are (a) 0 μM , (b) 4 μM , (c) 7 μM ,
205 and (d) 9 μM , respectively. Inset: the corresponding photographs. (B) Effect of S^{2-} on
206 the absorbance ratio (A_{680}/A_{520}) of sensing system. Inset: The linear relationship
207 between A_{680}/A_{520} and the concentration of S^{2-} . Conditions: pH: 9, TU concentration:
208 5 μM , and incubation time: 3 min.

209

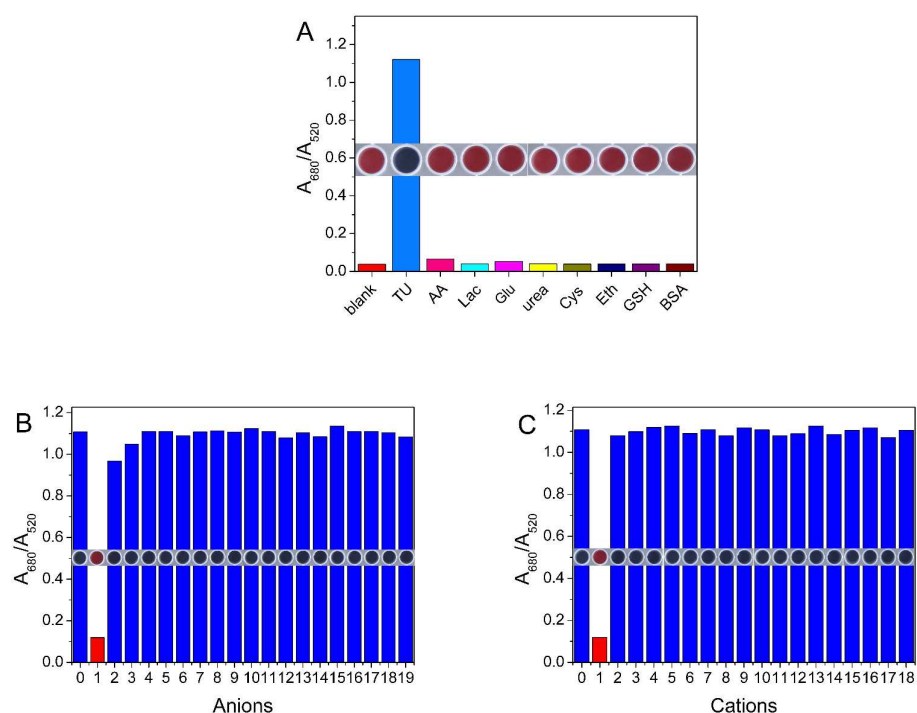
210

211 Selectivity

212 Selectivity is a very important parameter to estimate the performance of a sensor.
213 The selectivity of our constructed system involves two sides. On the one hand, to
214 check for false positive signals, various molecules, such as ascorbic acid (AA), lactose
215 (Lac), glucose (Glu), urea, cysteine (Cys), ethanol (Eth), bovine serum albumin (BSA)
216 and glutathione (GSH), were investigated to evaluate the selective response of TU
217 towards AuNPs. Fig. 4A shows visual color change and absorbance ratio of the
218 AuNPs in the presence of TU and other interferences. It is clearly observed that only
219 TU induced a dramatic color change from wine-red to blue but the others with
220 concentration of 20 times higher than that of TU could not induce the aggregation of
221 AuNPs. These results proved the distinct capability of our constructed system to avoid
222 producing false positive signals. On the other hand, to check for false negative signals,
223 we investigated the response of TU-AuNPs system in the presence of various ions. As
224 manifested in Fig. 4B and Fig. 4C, none of anions except for S^{2-} could prevent the TU
225 induced aggregation of AuNPs and most cations showed no interference for this

226 method. It's worth noting that under the conditions employed here, polysulfide fail to
 227 appear because sulfur is not being produced by oxygenation of sulfide when pH
 228 values are greater than 9.³⁰ Thus, the interference from polysulfide can be avoided.
 229 Cu^{2+} , Mn^{2+} , Al^{3+} and Fe^{3+} could interfere the assay at high concentration. However,
 230 with the help of EDTA, which is a strong metal ion chelator, the interferences from
 231 these cations with concentration of 10 times higher than that of S^{2-} can be ignored.
 232 These results demonstrated the excellent selectivity of this approach applied in S^{2-}
 233 detection.

234



235

236 **Fig. 4** (A) The colorimetric response of the sensing system in the absence and
 237 presence of AA, Lac, Glu, urea, Cys, Eth, BSA and GSH (100 μM each), as well as
 238 TU (5 μM). (B) The colorimetric response of the sensing system in the absence and
 239 presence of various anions. Samples marked with 0-19 corresponding to blank, S^{2-} ,
 240 $\text{S}_2\text{O}_3^{2-}$, I^- , SCN^- , $\text{S}_2\text{O}_8^{2-}$, SO_4^{2-} , SO_3^{2-} , Cl^- , F^- , Br^- , BrO_3^- , IO_3^- , ClO_4^- , Ac^- , NO_3^- , NO_2^- ,
 241 HPO_4^{2-} , CO_3^{2-} and EDTA^{2-} , respectively. (TU: 5 μM ; S^{2-} : 9 μM ; $\text{S}_2\text{O}_3^{2-}$: 9 μM , I^- : 45
 242 μM , other anions: 90 μM each); (C) The colorimetric response of the sensing system
 243 in the absence and presence of various cations. Samples marked with 0-18

244 corresponding to blank, S^{2-} , Cu^{2+} , Mn^{2+} , Al^{3+} , Fe^{3+} , K^+ , Na^+ , Ca^{2+} , Mg^{2+} , Fe^{2+} , Co^{2+} ,
 245 Ni^{2+} , Zn^{2+} , Ba^{2+} , Cd^{2+} , Pb^{2+} , NH_4^+ , and Cr^{3+} , respectively. (TU: 5 μM ; S^{2-} : 9 μM ; Al^{3+} :
 246 9 μM ; Fe^{3+} : 9 μM ; Cu^{2+} : 45 μM ; Mn^{2+} : 45 μM ; other cations: 90 μM each) Conditions:
 247 pH: 9, and incubation time: 3 min.

248

249 Logic sensing S^{2-} in real samples

250 Since most of the ions and molecules did not interfere, we believe that this logic
 251 gate will operate finely in the S^{2-} assay for relatively complex matrix systems. In order
 252 to illustrate this proposal, several real samples, including river water, mineral water,
 253 tap water, human urine, monosodium glutamate, sugar, and white wine, were
 254 employed as potential practical subjects containing S^{2-} . For all samples, both unspiked
 255 and spiked, the states of TU were "1". According to the results of the logic gate
 256 operation showed in Fig. 5, the states of output were "1" for all unspiked samples,
 257 indicating that no S^{2-} was detected (in the "0" state), while the states transformed to
 258 "0" for all samples after the standard spiking (in the "1" state), showing usefulness of
 259 the INHIBIT gate in the logic detection of S^{2-} in various practical samples.

260

261

262

263

264

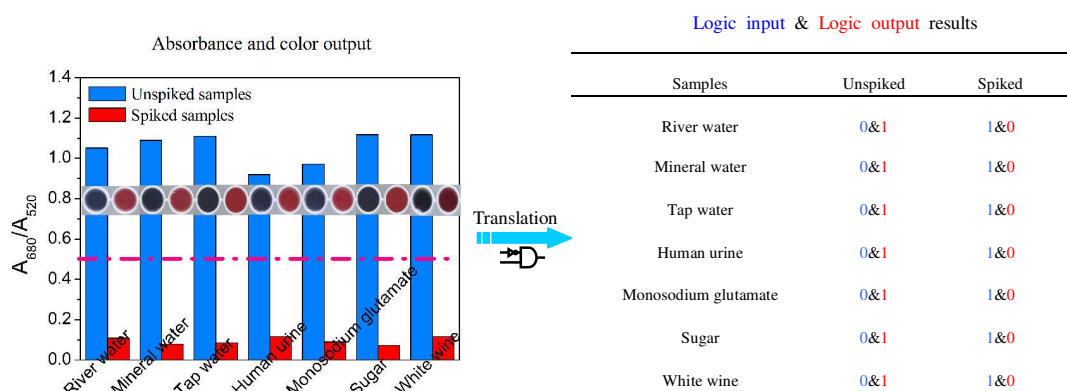
265

266

267

268

269



270 **Fig. 5** Application of the established INHIBIT logic gate for S^{2-} sensing in various
 271 real samples. The logic gate translates absorbance (left) and visual color (inset, left)
 272 outputs of unspiked and spiked samples to logical outputs and thence to logical input
 273 results, i.e. the presence of S^{2-} (right). For spiked samples, the concentrations of S^{2-}
 274 were all 10 μM . Conditions: pH: 9, TU concentration: 5 μM , and reaction time: 3 min.

275

276 **Conclusion**

277 In summary, we designed a noncommutative logic gate (INHIBIT gate) by utilizing
278 citrate-capped AuNPs as a signal transducer with sulfide and TU as mechanical
279 activators. Based on the logic gate, a colorimetric sensor was devised for inexpensive,
280 label-free, rapid, sensitive and selective determination of S^{2-} . The distinctive
281 advantage of this system is that recognition events can be translated into a color
282 change of the solution, which can be monitored by UV-visible spectroscopy or even
283 the naked eyes. Moreover, this logic gate was successfully applied for S^{2-} sensing in
284 various practical samples, implying its extensive applications in food, environment,
285 and biological system.

286

287 **Acknowledgement**

288 The authors gratefully acknowledge the financial support of the National Natural
289 Science Foundation of China (21175023), the Program for New Century Excellent
290 Talents in University (NCET-12-0618), the Science and Technology Planning Project
291 of Fujian Province (2012Y0028), the Medical Elite Cultivation Program of Fujian
292 Province (2013-ZQN-ZD-25), and the Medical Innovation Project of Fujian Province
293 (2014-CX-6).

294

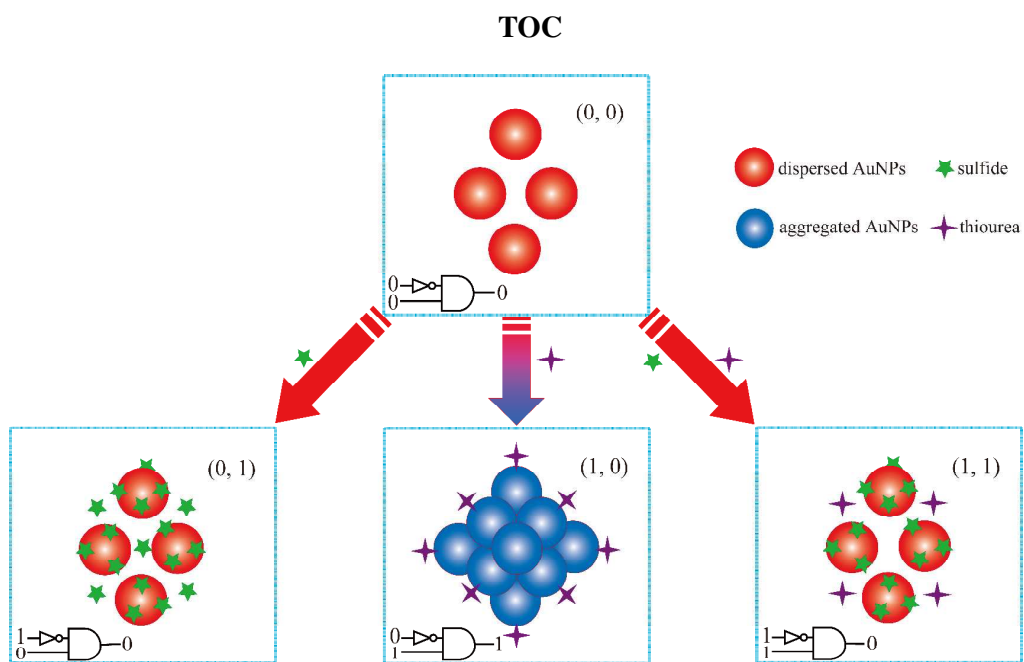
295 **References**

- 296 1. E. Blackstone, M. Morrison, M.B. Roth, *Science*, 2005, **308**, 518-518.
- 297 2. A. K. Mustafa, M. M. Gadalla, N. Sen, S. Kim, W. Mu, S. K. Gazi, R. K.
298 Barrow, G. Yang, R. Wang, S. H. Snyder, *Sci. Signal.*, 2009, **2**, ra72.
- 299 3. K. Eto, T. Asada, K. Arima, T. Makifuchi, H. Kimura, *Biochem. Biophys. Res.*
300 *Commun.*, 2002, **293**, 1485-1488.
- 301 4. P. Kamoun, M. C. Belardinelli, A. Chabli, K. Lallouchi, B. Chadefaux-Vekemans,
302 *Am. J. Med. Genet. A*, 2003, **116**, 310-311.
- 303 5. S. Balasubramanian, V. Pugalenti, *Water Res.*, 2000, **34**, 4201-4206.
- 304 6. X. Cao, W. Lin, L. He, *Org. Lett.*, 2011, **13**, 4716-4719.

- 305 7. Y. Dilgin, B. Kızılkaya, B. Ertek, N. Eren, D. G. Dilgin, *Talanta*, 2012, **89**,
306 490-495.
- 307 8. R. Huang, X. Zheng, Y. Qu, *Anal. Chim. Acta*, 2007, **582**, 267-274.
- 308 9. D. Jiménez, R. Martínez-Máñez, F. Sancenón, J. V. Ros-Lis, A. Benito, J. Soto,
309 *J. Am. Chem. Soc.*, 2003, **125**, 9000-9001.
- 310 10. Y. Jin, H. Wu, Y. Tian, L. Chen, J. Cheng, S. Bi, *Anal. Chem.*, 2007, **79**,
311 7176-7181.
- 312 11. F. Maya, J. M. Estela, V. Cerdà, *Anal. Chim. Acta*, 2007, **601**, 87-94.
- 313 12. B. Xiong, R. Zhou, J. Hao, Y. Jia, Y. He, E. S. Yeung, *Nature Commun.*, 2013,
314 **4**, 1708.
- 315 13. J. Zhang, X. Xu, X. Yang, *Analyst*, 2012, **137**, 1556-1558.
- 316 14. H. H. Deng, S. H. Weng, S. L. Huang, L. N. Zhang, A. L. Liu, X. H. Lin, W.
317 Chen, *Anal. Chim. Acta*, 2014, **852**, 218-222.
- 318 15. S. Bi, Y. Yan, S. Hao, S. Zhang, *Angew. Chem. Int. Ed.*, 2010, **122**, 4540-4544.
- 319 16. R. Orbach, L. Mostinski, F. Wang, I. Willner, *Chem.-Eur. J.*, 2012, **18**,
320 14689-14694.
- 321 17. Y. Jiang, N. Liu, W. Guo, F. Xia, L. Jiang, *J. Am. Chem. Soc.*, 2012, **134**,
322 15395-15401.
- 323 18. J. Ren, J. Wang, J. Wang, E. Wang, *Chem.-Eur. J.*, 2013, **19**, 479-483.
- 324 19. X. Xu, J. Zhang, F. Yang, X. Yang, *Chem. Commun.*, 2011, **47**, 9435-9437.
- 325 20. B. C. Yin, B. C. Ye, H. Wang, Z. Zhu, W. Tan, *Chem. Commun.*, 2012, **48**,
326 1248-1250.
- 327 21. J. Du, S. Yin, L. Jiang, B. Ma, X. Chen, *Chem. Commun.*, 2013, **49**, 4196-4198.
- 328 22. D. Liu, W. Chen, K. Sun, K. Deng, W. Zhang, Z. Wang, X. Jiang, *Angew. Chem.*
329 *Int. Ed.*, 2011, **50**, 4103-4107.
- 330 23. Y. Xianyu, Z. Wang, J. Sun, X. Wang, X. Jiang, *Small*, 2014, **10**, 4833-4838.
- 331 24. H. H. Deng, G. W. Li, X. H. Lin, A. L. Liu, W. Chen, X. H. Xia, *Analyst*, 2013,
332 **138**, 6677-6682.
- 333 25. S. Wang, W. Chen, A. L. Liu, L. Hong, H. H. Deng, X. H. Lin, *ChemPhysChem*,
334 2012, **13**, 1199-1204.

- 335 26. R. Jin, G. Wu, Z. Li, C. A. Mirkin, G. C. Schatz, *J. Am. Chem. Soc.*, 2003, **125**,
336 1643-1654.
- 337 27. S. Mallick, S. Mondal, B. K. Bera, P. Karmakar, S. C. Moi, A. K. Ghosh,
338 *Transit. Metal Chem.*, 2010, **35**, 469-475.
- 339 28. K. S. Park, M. W. Seo, C. Jung, J. Y. Lee, H. G. Park, *Small*, 2012, **8**,
340 2203-2212.
- 341 29. A. P. de Silva, N. D. McClenaghan, *Chem.-Eur. J.*, 2004, **10**, 574-586.
- 342 30. K. Y. Chen, J. C. Morris, *Environ. Sci. Technol.*, 1972, **6**, 529-537.
- 343

344



345

346 An INHIBIT logic gate is designed based on citrate-capped gold nanoparticles and

347 successfully utilized to the determination of sulfide.